Time Response of the High-field Electron Distribution Function in GaAs

Abstract: Numerical calculations have been made of the high-field electron distribution function for GaAs, its small-signal frequency response and its behavior in large sinusoidal electric fields. The response speed is limited by the low scattering rate within the (000) valley. With increasing frequency the threshold field for negative conductivity rises and the negative mobility and oscillator efficiency fall. The free-electron dielectric constant is positive at high fields, with a peak near the threshold field.

Introduction

In recent years, devices such as the Gunn diode and the avalanche diode, whose characteristics are determined by the behavior of electrons in high electric fields, have become increasingly important. These developments have greatly increased the need for a technique for analyzing realistically the behavior of free carriers in high electric fields. The standard semiclassical method for tackling transport problems is to attempt to solve the Boltzmann equation, but this method becomes difficult for realistic band structures and scattering processes. Usually it is necessary to introduce approximations by assuming some parametric form for the electron distribution function, such as a displaced Maxwellian distribution. The parameters are then adjusted to give a best fit to the Boltzmann equation. The weaknesses of this technique are the lack of generality of any one type of approximation and the difficulty of assessing the consequences of the approximations.

Recently, two numerical methods, one a Monte Carlo^{2, 3} and the other an iterative method⁴ have been developed for calculating free-carrier distribution functions without needing to assume any a priori form for the distribution function. Both methods assume the same semiclassical picture of the electron motion as is implicit in the Boltzmann equation. Provided the band structure and scattering rates are known, they permit the numerical calculation of steady-state distribution functions, and hence velocity-field curves, without further approximation. They are therefore particularly suited to complex problems for which analytic techniques fail and the use of parametric distribution

The iterative method has been used to calculate the electron distribution function in GaAs, and hence the electron drift velocity, in both steady and time-varying electric fields. The results are of practical significance in view of the extensive exploitation in microwave frequency oscillators of the negative differential conductivity exhibited by n-type GaAs for fields above about 3 kV/cm.

In the next two sections the techniques used to calculate the steady-state and time-dependent electron distribution functions in GaAs are outlined. Following sections deal, respectively, with the small- and large-signal frequency response of the electron distribution. In each case it is assumed that the electron distribution is spatially uniform, so that space charge accumulation and effects of diffusion are neglected. The calculations, which extend some early results reported previously, 5 concentrate on the frequency range from dc to about 100 GHz, which includes the range of main device interest.

Method of computation

It can be shown⁴ that the steady-state distribution function $f(\mathbf{k})$ for electrons in an electric field \mathbf{F} may be generated by an iterative process. The *n*th iterate $f_n(\mathbf{k})$ is derived from the (n-1)th by two stages of integration. The first stage is to derive a function $g(\mathbf{k})$ by the relation

$$g(\mathbf{k}') = \int d\mathbf{k} f_{n-1}(\mathbf{k}) S(\mathbf{k}, \mathbf{k}'), \qquad (1)$$

H. D. Rees is with the Royal Radar Establishment, Malvern, Worcestershire, England.

537

functions is dubious. A special property of the iterative method is that it can be modified so that each iteration becomes equivalent to a time step of the physical system.⁴ This permits the calculation of time-dependent as well as steady-state distribution functions, and hence the response of the electrons to time-varying fields may be derived.

where $S(\mathbf{k}, \mathbf{k}')$ is the scattering rate from \mathbf{k} to \mathbf{k}' . The second stage may be expressed as

$$f_{n}(\mathbf{k}) = \int_{0}^{\infty} dt \ g(\mathbf{k} - e\mathbf{F}t/\hbar)$$

$$\times \exp\left\{-\int_{0}^{t} \lambda(\mathbf{k} - e\mathbf{F}t/\hbar + e\mathbf{F}t'/\hbar) \ dt'\right\},$$
(2)

where $\lambda(\mathbf{k})$ is the total scattering rate, obtained by integrating $S(\mathbf{k}, \mathbf{k}')$ over all final states \mathbf{k}' .

The first important property of the iterative process is that, for large enough values of n, successive iterates converge to the steady-state distribution function irrespective of the form of the starting function $f_0(\mathbf{k})$. A second property, which permits time-dependent problems to be analyzed, is that incorporation in $S(\mathbf{k}, \mathbf{k}')$ of an additional non-physical scattering process, referred to as self scattering, of the form

$$[\Gamma - \lambda(\mathbf{k})]\delta(\mathbf{k} - \mathbf{k}'), \tag{3}$$

makes each iteration approximately equivalent to a time step of magnitude $1/\Gamma$. For convergence Γ must be chosen larger than the largest value of $\lambda(k)$. By increasing the value of Γ , one can make the time-step approximation arbitrarily accurate.

The detailed numerical method for carrying out the iteration in the present calculations is only one of many possibilities. In outline it proceeds as follows. The first part of each iteration, represented by (1), is carried out using spherical polar coordinates, which exploits very effectively the overall energy conservation for each scattering process. Equation (1) is evaluated by accumulating the contributions due to each scattering process in turn [e.g., polar phonon, intervalley phonon and the self-scattering term corresponding to (3)].

When the self-scattering term (3) is incorporated in the scattering rate, Eq. (2) reduces to

$$f_n(\mathbf{k}) = \int_0^\infty dt \ g(\mathbf{k} - e\mathbf{F}t/\hbar) \ \exp(-\Gamma t). \tag{4}$$

The second part of each iteration, comprising the evaluation of (4) as a function of **k**, is most simply carried out using cylindrical polar coordinates in **k**, with the reference axis parallel to the electric field. In order that each stage of the iteration may be carried out in the most convenient coordinate system, spherical polar to cylindrical polar coordinate changes are made between alternate stages.

The small-signal response of the electrons is found by calculating the response to a small step of electric field. The step response can then be transformed to yield the frequency response. There is no simple way of estimating in advance the value of Γ that is required to yield an adequate description of the time response, and in practice

the smallest acceptable value is found by trial. (An unnecessarily large Γ wastes computer time since the number of iterations increases in proportion to Γ .)

The large-signal responses, which are here confined to calculations for sinusoidally varying electric fields, are derived by resetting the value of the electric field for each iteration. The required field change is, of course, that appropriate to a time step $1/\Gamma$.

GaAs parameters

The model of the GaAs band structure and scattering rates is the same as that used for earlier calculations. The simplifications introduced by this model are, of course, the factors limiting the validity of the calculations.

The $\langle 000 \rangle$ and the three degenerate $\langle 100 \rangle$ conductionband valleys are assumed to be spherical and parabolic with effective mass 0.067 and 0.35 times the free electron mass, respectively. The scattering rates are the standard expressions derived from first-order perturbation theory. The only intravalley scattering processes included are optical polar phonon and acoustic phonon scattering, impurity and defect scattering being omitted. For intervalley scattering, the deformation potential was taken to be 10⁹ eV-cm⁻¹, both for scattering between the central and satellite valleys and among the equivalent satellite valleys. The present choice for the satellite valley effective mass and for the deformation potential for the scattering between central and satellite valleys has been shown to yield a more satisfactory static characteristic than the parameters used for calculations employing displaced Maxwellian distribution functions. Monte Carlo calculations have shown that the parabolic-band approximation yields a static characteristic very similar to that obtained when account is taken of non-parabolicity and the variation with k of the Bloch functions. This suggests that the present model should describe quite well all the main features of the electron behavior in GaAs.

The static characteristic for fields up to 16 kV/cm is shown in Fig. 1. The value of Γ used for the computations was $2.5 \times 10^{13} \text{ sec}^{-1}$, the smallest value ensuring convergence. Typically, each iteration required computer time equivalent to about 10^5 multiplications and convergence to the steady-state distribution was obtained after about 100 iterations. This value of Γ was found by trial to be adequate for evaluation of time responses.

Small-signal response

In the first place, attention is confined to the response of the electrons to an incremental field parallel to the dc electric field. Figure 2 shows the time response of the central valley velocity v_1 , the satellite valley velocity v_2 , the satellite valley population fraction n_2 , and the drift velocity v, when the electric field is stepped from 6 to 5 kV/cm. The satellite valley velocity readjusts in less than

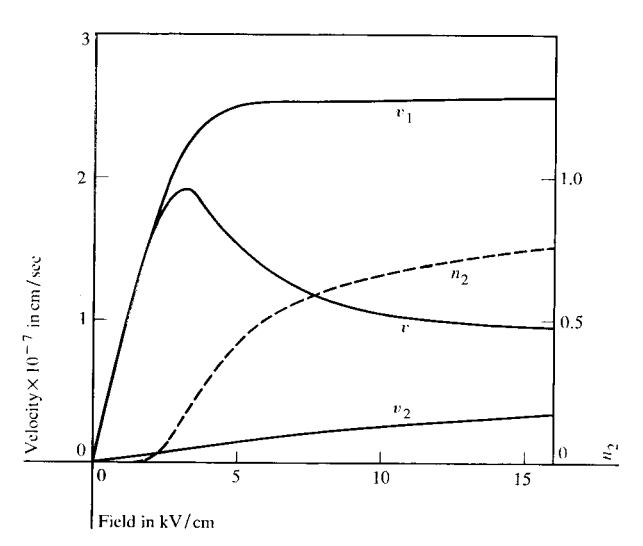


Figure 1 Static characteristic for n-GaAs; v_1 , v_2 , v are central valley, satellite valley and drift velocity, respectively n_2 is the satellite valley population fraction.

 10^{-13} sec, reflecting the short scattering times for the satellite valleys. By contrast, v_1 falls for about 4×10^{-13} sec and then recovers over a period of order 5×10^{-12} sec. The transfer of electrons from the satellite to the central valleys, indicated by the n_2 curve, is also slow. Clearly the overall response speed of the distribution is limited by scattering processes within the central valley. This reflects the weak scattering of electrons in the central valley with kinetic energies between about 0.1 eV, below which polar phonon scattering is strong, and about 0.35 eV, above which intervalley scattering is strong.

The response of the drift velocity v shows an initial drop, followed by an increase due partly to the intervalley transfer and partly to the recovery of v_1 . The final velocity exceeds the initial velocity, illustrating the negative differential conductivity of the electrons.

The step response indicated in Fig. 2 provides a reasonable approximation to the small-signal step response for a bias field of 5.5 kV/cm, which is the mean of the initial and final fields. Fourier transformation of the drift-velocity step response yields the frequency response of the smallsignal mobility shown in Fig. 3. The component of mobility in phase with the field is negative at low frequencies, but increases with frequency and is positive above 80 GHz, reflecting the short time response of the drift velocity. It is worth emphasizing that the positive differential mobility at high frequencies is a direct consequence of the response of the central valley velocity in phase with the field, which more than compensates for the in-phase component of n_2 that persists even at high frequencies. The quadrature component of the differential mobility indicates that the electrons act capacitatively. The corresponding

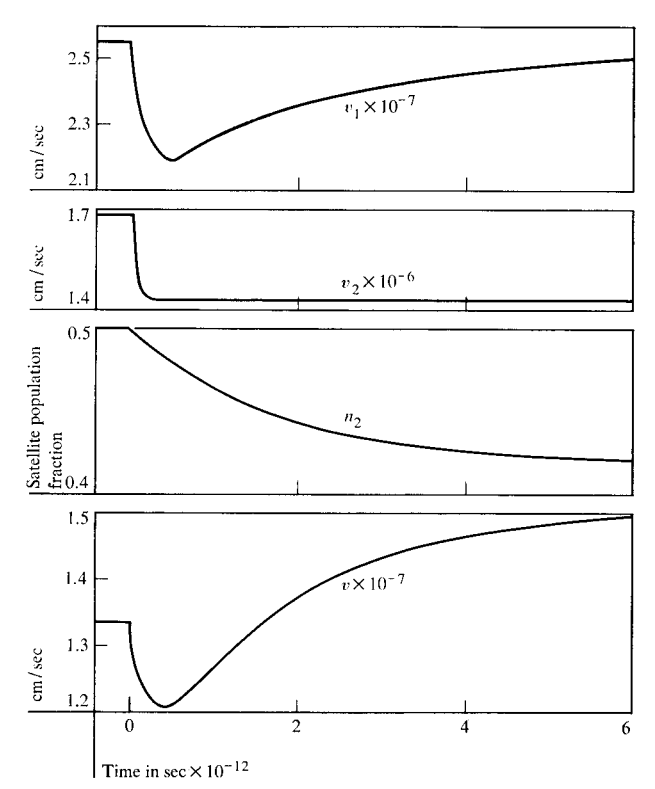
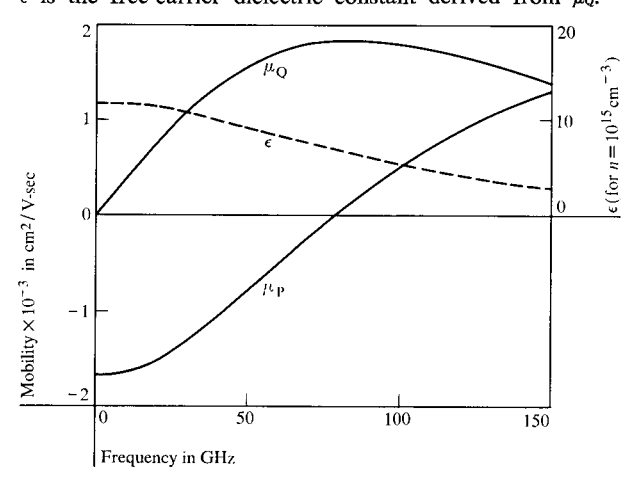


Figure 2 Response of electrons to a field stepped from 6 to 5 kV/cm at time t = 0.

Figure 3 Frequency dependence of differential mobility for a bias field of 5.5 kV/cm; μ_P and μ_Q are respectively the components in phase and quadrature with the ac field and ϵ is the free-carrier dielectric constant derived from μ_Q .



free-carrier contribution to the dielectric constant, calculated for an electron density of 10¹⁵ cm⁻³, is also shown in Fig. 3.

The next consideration is the dependence of the differential mobility on the bias field. Figure 4 shows the frequency dependence of the phase component of the differential mobility for a series of bias fields. The curve for

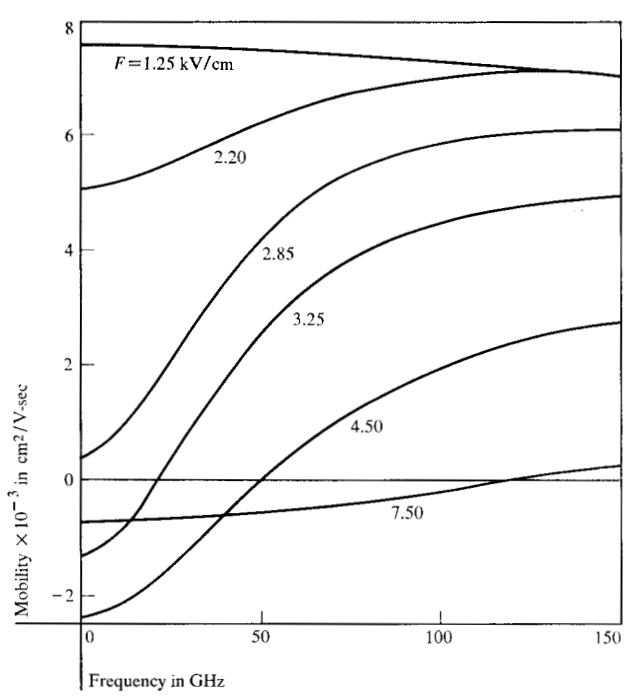


Figure 4 Frequency dependence of differential mobility for several bias fields.

1.25 kV/cm is representative of the behavior below about 2 kV/cm. For these low fields an insignificant fraction of the electrons has kinetic energy in excess of 0.1 eV, and so all the electrons are strongly scattered by the polar phonons. Consequently, the mobility shows only a weak frequency dependence; the slight reduction at high frequencies reflects a momentum relaxation time of about 3×10^{-13} sec. Above about 2 kV/cm the electron response is dominated by the effects described previously, and the differential mobility shows the characteristic rise with frequency. With a further increase of bias field, the electrons are accelerated more rapidly through the weak-scattering region, which causes the overall response speed to rise. Therefore, as may be seen from the curves of Fig. 4, the frequency dependence of the mobility becomes less at higher bias fields. Consequently, for increasing frequency there is an increase of the effective threshold field as well as a decrease of the negative differential mobility.

The conclusions are summarized in Fig. 5 which shows the frequency dependence of the effective threshold field F_0 , the bias field F_m at which the negative mobility is greatest, and the maximum value μ_m of the negative mobility. While calculations of the small-signal conductivity provide only a general guide to the expected performance of microwave oscillators, the results indicate that high-frequency operation is possible only for fields well above the low-frequency threshold and that the efficiency should fall with frequency. The smallness of the

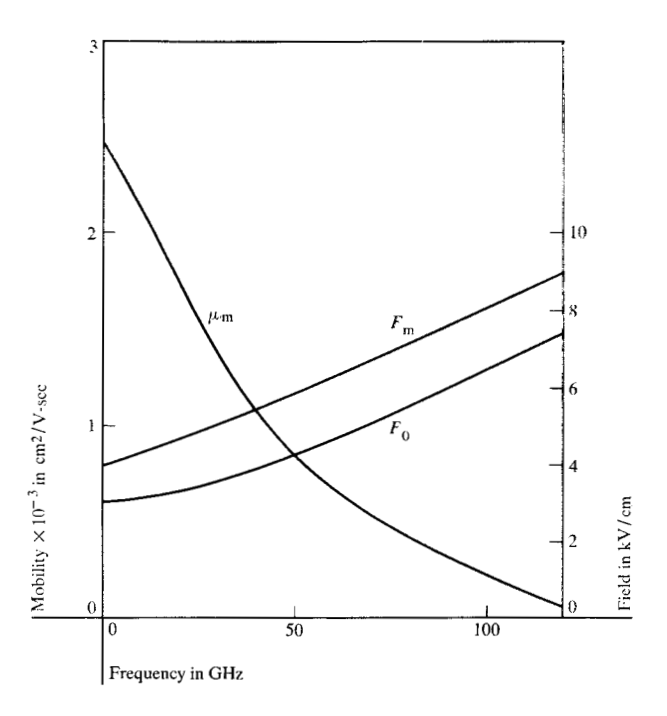


Figure 5 Frequency dependence of F_0 (threshold field), F_m (field for maximum negative mobility) and μ_m (maximum negative mobility).

negative mobility above 100 GHz suggests that the maximum frequency (of the first harmonic) of a GaAs oscillator is in this region.

The behavior of the quadrature component of the differential mobility is illustrated in Fig. 6, which shows the free-carrier dielectric constant for an electron density of 10¹⁵ cm⁻³ as a function of bias field. Below about 2 kV/cm, the electron distribution is only slightly heated and the electrons act inductively, but at higher fields they act capacitatively. From the microwave device viewpoint, there are two interesting consequences of the free-carrier dielectric constant of n-GaAs. First, for the usual range of electron densities of 10¹⁵ to 10¹⁶ cm⁻³, the typical freecarrier dielectric constant will exceed the lattice dielectric constant of 12.53, and so will substantially increase the device capacitance. Second, the sharp peak of the freecarrier dielectric constant indicates that the electrons will act as a nonlinear capacitance. This introduces the possibility of parametric generation of subharmonics of oscillator frequencies, which may be relevant to the reported subharmonic generation from an LSA X-band oscillator.

The final aspect of the present analysis of the small-signal response is to consider the behavior of the electrons when the incremental field is transverse to the bias field. The results of the calculations are summarized in Fig. 7, which shows the frequency dependence of the phase component of the transverse differential mobility for bias fields of 0, 1.5, 6 and 15 kV/cm. In contrast to a parallel

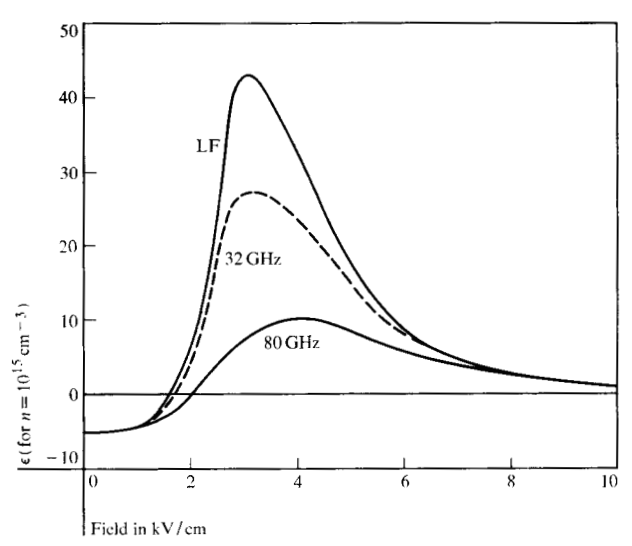


Figure 6 Dependence of free-carrier dielectric constant on bias field for low frequency (LF), 32 and 80 GHz.

incremental field, a transverse incremental field produces no heating; its effects are confined to changing electron momentum direction. Consequently, the low-frequency transverse differential mobility has the same value as the dc mobility at the bias field. Processes tending to change the energy distribution of the electrons are absent and therefore the response of the distribution to the incremental field is much faster. The results of Fig. 7 bear out these conclusions. The mobility falls slowly with frequency; the corresponding quadrature component of mobility is inductive, but very small at both low and high bias fields.

Large-signal response

The present calculations are restricted to problems in which there is no spatial variation of the electron distribution. The only mode of operation of microwave oscillators for which this condition is valid is the LSA mode, which is therefore of special interest. The small-signal calculations show that the behavior of microwave oscillators at frequencies greater than about 20 GHz will differ markedly from that predicted on the assumption that the static velocity-field characteristic is followed at high frequencies. However, these calculations cannot be compared in detail with LSA oscillator behavior since the LSA mode is a large-signal mode, which makes it desirable to carry out large-signal computations of the electron response.

For the static characteristic, part of which is shown in Fig. 1, an ac field of 8 kV/cm peak superimposed on a dc field of 10 kV/cm gives a calculated low-frequency efficiency of 14.5%, which is near the maximum, and satisfies the condition of net space-charge decay over a complete cycle. The response of the electron distribution to this field waveform has been calculated for frequencies of 30

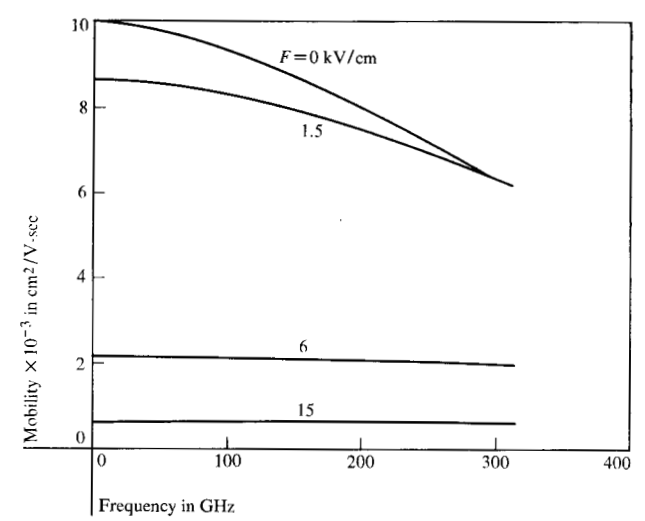
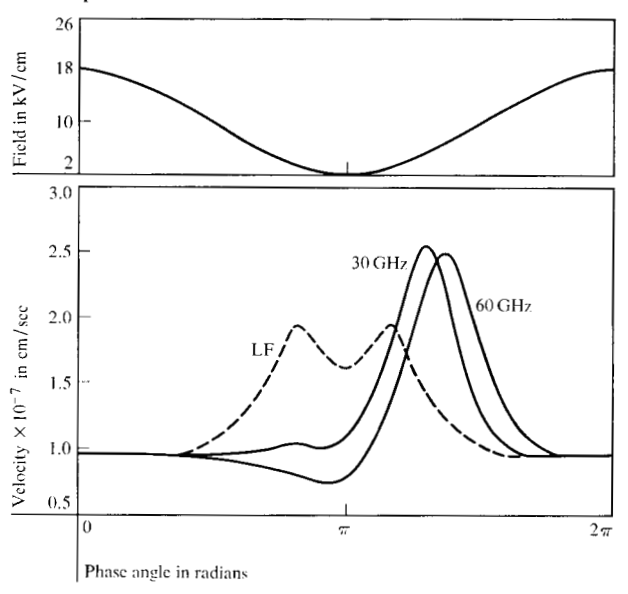


Figure 7 Frequency dependence of transverse differential mobility for several bias fields.

Figure 8 Response of electron drift velocity to 8 kV/cm ac field with 10 kV/cm dc bias field at low frequency (LF), 30 and 60 GHz. The upper curve shows the electric field and the lower curves shows the velocity as functions of the ac phase.



and 60 GHz, and the derived electron velocities, plotted as functions of ac phase, are compared in Fig. 8 with the corresponding low-frequency velocity derived from the static characteristic.

The most obvious consequence of increasing frequency is an increasing phase shift of the electron velocity, which reflects the capacitative response of the electrons. Fourier analysis of the waveforms of Fig. 8 shows that the average free-carrier dielectric constant (derived from the quadrature part of the fundamental velocity component) for an electron concentration of 10¹⁵ cm⁻³ is 19 at 30 GHz and

13 at 60 GHz. The corresponding low-frequency value is 30. It is clear that, for many devices, the free-carrier contribution to the device capacitance will be at least comparable to the lattice contribution. The decrease of the free-carrier dielectric constant with frequency reflects the similar small-signal behavior indicated by Fig. 6. The oscillator efficiency, also derived from the Fourier analysis of the velocity waveforms, shows the expected fall with frequency, being 9.5% at 30 GHz and 3.5% at 60 GHz compared with the low-frequency value of 14.5%. A roughly similar decrease of efficiency with frequency has been obtained on the assumption of displaced Maxwellian distribution functions.⁷

The increase of response speed with bias predicted by the small-signal analysis is reflected by the large-signal behavior. As the electric field falls from its maximum of 18 kV/cm to about 10 kV/cm, the electron distribution remains close to the steady distribution that would obtain at the same field, i.e., the electron distribution follows the field adiabatically. At lower fields the electron response becomes progressively slower and, as may be seen from the curves of Fig. 8, the distribution below 5 kV/cm is quite different from the corresponding static distribution. With increasing field, the distribution corrects itself, attaining essentially the static form at a field of about 11 kV/cm at 30 GHz and 15 kV/cm at 60 GHz. The fact that the electron distribution behaves adiabatically at the higher fields, but fails to adjust to the static value at lower fields, causes a small drop in the dc current. At 60 GHz the calculated dc current is about 8% below that for lowfrequency oscillation.

Conclusions

The present distribution-function calculations are directed at analyzing the fundamental behavior of electrons in GaAs, particularly the response of the electrons to field variations. An important justification for the computational effort is the desirability of improving the understanding of the operation of GaAs transferred-electron microwave oscillators. Therefore the calculations are mainly concerned with the frequency range from low frequency to about 100 GHz.

It is immediately apparent from the computed results that the basic response of the electrons varies greatly through the frequency range up to $100~\rm GHz$. The response speed is dictated by the weakness of the scattering of electrons in the $\langle 000 \rangle$ valley, which have kinetic energies greater than about $0.1~\rm eV$ (below which polar scattering is strong) and less than about $0.35~\rm eV$ (above which intervalley scattering is strong). The response to transverse incremental electric fields is very much faster than the parallel response, a behavior which may be qualitatively described by long effective energy relaxation times.

With increasing frequency the negative differential mobility falls and the effective threshold field rises. At 50 GHz the maximum negative mobility is only about 35% of that for low frequencies, and the threshold field has increased from 3 to 4.5 kV/cm. The general expectation of a fall of oscillator efficiency with frequency is supported by large-signal calculations showing, for one particular LSA mode, an efficiency of 3.5% at 60 GHz compared with the corresponding low-frequency value of 14.5%.

The free-carrier contribution to the dielectric constant of GaAs is of potential device significance for two reasons: First, for electron concentrations in excess of 10¹⁵ cm⁻³, the free-carrier dielectric constant is substantially greater than the lattice dielectric constant, and therefore may have noticeable tuning effects. Second, the free-carrier dielectric constant is sharply peaked near 3 kV/cm, and consequently the electrons can act as a nonlinear reactance. This immediately introduces the possibility of parametric generation of low-frequency power in high-frequency oscillators, which is of obvious relevance to device operation.

In the wider context of semiconductor transport problems, techniques such as those used here can, at the expense of needing numerical evaluation, provide accurate solutions to problems of realistic complexity. The present calculations are restricted to spatially uniform distributions, but the computational techniques can be adapted to spatially variable problems. Similarly, magnetic as well as electric fields can be incorporated.

Techniques with these capabilities are essential for a quantitative evaluation of the transport of electrons in real semiconductors and therefore, to give an important example, should assist the understanding of the operation of hot-electron devices.

Acknowledgments

The author acknowledges valuable discussions with T. P. McLean and W. Fawcett and is indebted to J. B. Arthur, who wrote a special section of the computer program.

References

- P. N. Butcher and W. Fawcett, *Phys. Letters* 21, 489 (1966).
- T. Kurosawa, (Proc. Int. Conf. Phys. Semiconductors, Kyoto, 1966) J. Phys. Soc. Japan (Supplement) 21, 424 (1966).
- A. D. Boardman, W. Fawcett and H. D. Rees, Solid State Comm. 6, 305 (1968).
- 4. H. D. Rees, J. Phys. Chem. Solids 30, 643 (1969).
- 5. H. D. Rees, Solid State Comm. 7, 267 (1969).
- 6. R. H. Chilton, Proc. IEEE 56, 1124 (1968).
- P. N. Butcher and C. J. Hearn, Electronics Letters 4, 459 (1968).

Received April 8, 1969